

# BIMODALITY IN SPECTATOR FRAGMENTATION

W. Trautmann<sup>(a)</sup> and the ALADIN Collaboration

<sup>(a)</sup> *Gesellschaft für Schwerionenforschung (GSI),  
Planckstr. 1, D-64291 Darmstadt, Germany*

## Abstract

The fluctuations of the largest fragment charge of a partition and of the charge asymmetries of the two or three largest fragments in spectator decays following  $^{197}\text{Au} + ^{197}\text{Au}$  collisions at 1000 MeV per nucleon are investigated. The observed bimodal distributions at specific values of the sorting variable  $Z_{\text{bound}}$  exhibit features known from percolation theory where they appear as finite-size effects. The underlying configurational fluctuations seem generic for fragmentation processes in small systems.

## 1 Introduction

Double-humped event distributions have received particular interest recently because their observation might indicate bimodality which is one of the signals expected for a first-order phase transition in finite systems [1-3]. Bimodality occurs when non-negligible surface interactions at the phase boundary lead to a convex entropy function in the transition region. Canonical sampling near the transition temperature will then produce two distinct event classes which differ with respect to the order parameter of the transition.

Bimodality has, e.g., been observed in solid-liquid transitions of clusters of Na atoms [4]. In these experiments, the clusters were thermalized in a heat bath of helium gas and excited with photons from a laser beam. Corresponding experiments in nuclear fragmentation face the difficulty that the temperature cannot be predetermined and that a canonical sampling can thus not be performed. There is, furthermore, the possibility of impact-parameter mixing, meaning that fluctuations of the variables used for sorting will unavoidably lead to finite distributions with respect to other observables or event characteristics (e.g., impact parameter) even in narrowly selected event samples. It is, nevertheless, of interest to study the origin and the meaning of bimodal event distributions and the conditions under which they occur. For example, Lopez et al. using the HIPSE event generator have recently pointed to the role of angular momentum in producing bimodal distributions as a result of instabilities of nuclei with high spin [5]. Pichon et al. [3] have shown that the two bumps of the bimodal distributions observed in  $^{197}\text{Au} + ^{197}\text{Au}$  fragmentations at 60 to 100 MeV per nucleon correspond to different scaling properties of the distributions of the largest fragment charge ( $\Delta$ -scaling [6]).

In this work, the fluctuations of the largest fragment charge of a partition and of the charge asymmetries of the two or three largest fragments from the decay of excited projectile spectators in  $^{197}\text{Au} + ^{197}\text{Au}$  collisions at 1000 MeV per nucleon are investigated. The data have been collected in experiments performed with the ALADIN spectrometer at GSI. The observed bimodal distributions at specific values

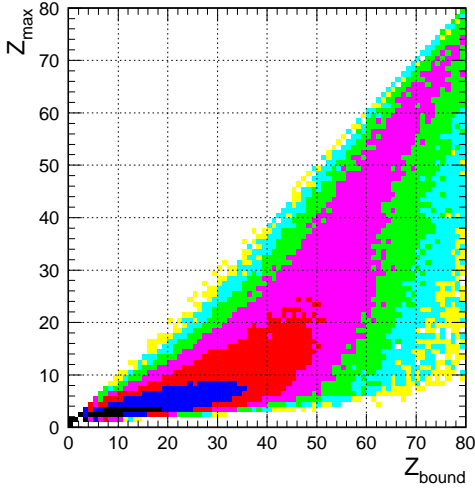


Figure 1: Distribution of  $Z_{\max}$  versus  $Z_{\text{bound}}$  for projectile fragments from  $^{197}\text{Au}$  on  $^{197}\text{Au}$  at 1000 MeV per nucleon [15]. Conventional fission events are removed. The shadings follow a logarithmic scale.

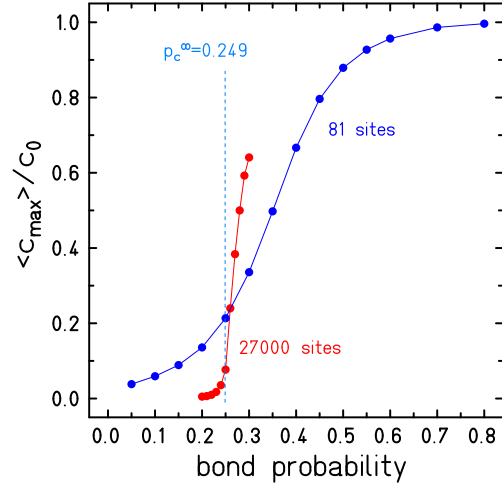


Figure 2: Bond percolation: mean relative magnitude of the largest cluster as a function of the bond probability for cubic lattices of  $c_0 = 81$  and 27000 sites. The critical bond probability in the infinite system is  $p_c^\infty = 0.249$ .

of the sorting variable  $Z_{\text{bound}}$  exhibit features known from percolation theory where they appear as finite-size effects. Percolation on a large lattice exhibits signatures of a second-order phase transition [7]. The observed similarities thus raise the question whether bimodality in fragmentation reactions may be used to infer the order of the phase transition in the nuclear case.

Bimodality and its significance for the interpretation of fragmentation data and their relation to the nuclear liquid-gas phase transition have been frequently discussed at previous conferences of this series [8-12]. At this year's conference, new results obtained by the INDRA collaboration are presented by E. Bonnet [13].

## 2 Experimental results

The data used for the present analysis were obtained by the ALADIN collaboration in measurements using  $^{197}\text{Au}$  projectiles of 1000 MeV per nucleon delivered by the heavy-ion synchrotron SIS at GSI [14, 15]. The ALADIN spectrometer was used to detect and identify the products of the projectile-spectator decay following collisions with  $^{197}\text{Au}$  target nuclei.

The sorting variable  $Z_{\text{bound}}$  is defined as the sum of the atomic numbers  $Z_i$  of all projectile fragments with  $Z_i \geq 2$ . It reflects the variation of the charge of the primary spectator system and is monotonically correlated with the impact parameter of the reaction [16]. The evolution of the dominant reaction processes is illustrated in Fig. 1 which shows the correlation of the largest atomic number  $Z_{\max}$  observed in a partition with  $Z_{\text{bound}}$ . Large values of  $Z_{\text{bound}}$  correspond to low excitation energies, at which the decay changes its character from evaporation-like processes ( $Z_{\max} \approx Z_{\text{bound}}$ ) to multifragmentation ("rise" of multifragmentation)

while small values correspond to reaction channels with high excitation energies and disintegrations into predominantly very light clusters ("fall" of multifragmentation,  $Z_{\max} \ll Z_{\text{bound}}$ ).

Besides the evolution of the mean and of the fluctuations of  $Z_{\max}$  (alternatively denoted by  $Z_1$  in the following) also those of two-fragment and three-fragment asymmetries are of interest and characterize the dominant transition of the reaction mechanism [17]. It is found that the ratios  $\langle Z_2/Z_1 \rangle$  and  $\langle Z_3/Z_2 \rangle$  both approach  $\approx 0.6$  at small  $Z_{\text{bound}}$  ( $Z_2$  and  $Z_3$  are the second and third largest atomic number  $Z$  of a partition). Consequently, the charge difference  $Z_1 - Z_2 - Z_3$ , or the corresponding asymmetry after normalizing with respect to the system charge  $Z_0$ , will approach zero at small  $Z_{\text{bound}}$  while it is close to  $Z_0$  (the asymmetry close to 1) at large  $Z_{\text{bound}}$ . In the transition region, the fluctuations of these observables are large [17] and the distributions are bimodal, i.e. they exhibit a two-hump structure (Fig. 3). Note that  $\langle Z_{\max} \rangle$  drops most rapidly in the bin  $53 < Z_{\text{bound}} \leq 57$  at which this bimodality is most strongly pronounced (Fig. 1).

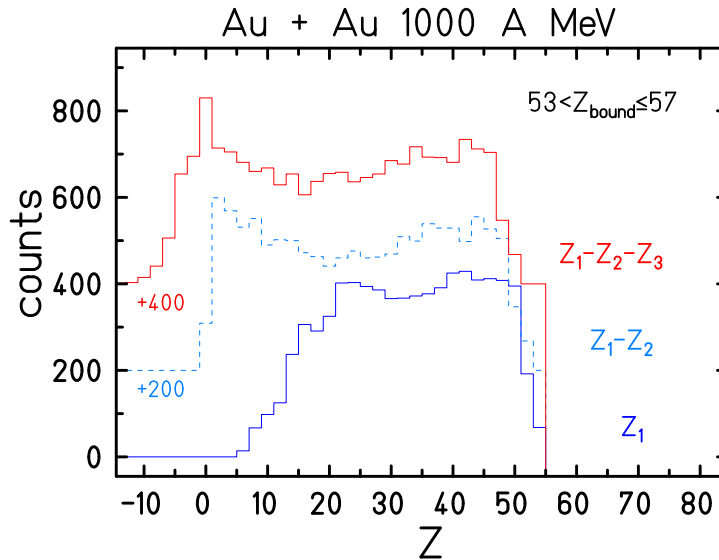


Figure 3: Distributions of the atomic number  $Z_1$  of the largest fragment of a partition and of the differences  $Z_1 - Z_2$  and  $Z_1 - Z_2 - Z_3$  for events with  $53 < Z_{\text{bound}} \leq 57$  from the fragmentation of  $^{197}\text{Au}$  projectiles at 1000 MeV per nucleon. Note the offsets by 200 and 400 counts of the difference distributions.

### 3 Largest fragment as order parameter

In the search for an experimentally accessible order parameter of the nuclear liquid-gas phase transition, as observed in multifragmentation reactions, the magnitude of the largest fragment of the partition has appeared as a promising choice. It may be identified with the part of the system in the liquid phase, and it is correlated with the mean density which is the natural order parameter of a liquid-gas phase transition. Observables correlated with it, as e.g. the differences and asymmetries discussed above, may similarly serve as order parameters.

Statistical model calculations for nuclear multifragmentation show that the disappearance of the dominating fragment is associated with a maximum of the heat capacity which is the more strongly pronounced the larger the system [18]. For  $A_0 = 150$ , the system mass for  $Z_{\text{bound}} \approx 50$  [14], the predicted specific heat distribution is rather wide with a maximum at  $T \approx 6.3$  MeV. This transition temperature, or boiling temperature according to the authors of [18], is comparable with values of the double-isotope temperature  $T_{\text{HeLi}}$  as measured for the present reaction [14, 19] and for similar systems [20]. The good description of the charge correlations and charge asymmetries characterizing the partitioning of the system, including their variances, with statistical multifragmentation models provides further evidence for the first-order nature of the transition [19, 21]. Bimodality is predicted for canonical ensembles [22, 23].

The disappearance of the largest cluster, with the variation of a suitable control parameter, has been identified as a prominent signal also in fragmentations of other systems as, e.g., atomic hydrogen clusters [24], and the extension of the largest cluster is an order parameter in percolation theory [7]. On finite percolation lattices, the disappearance of a dominant largest cluster proceeds rather smoothly and with obvious similarity to the nuclear experiment (Figs. 1,2).

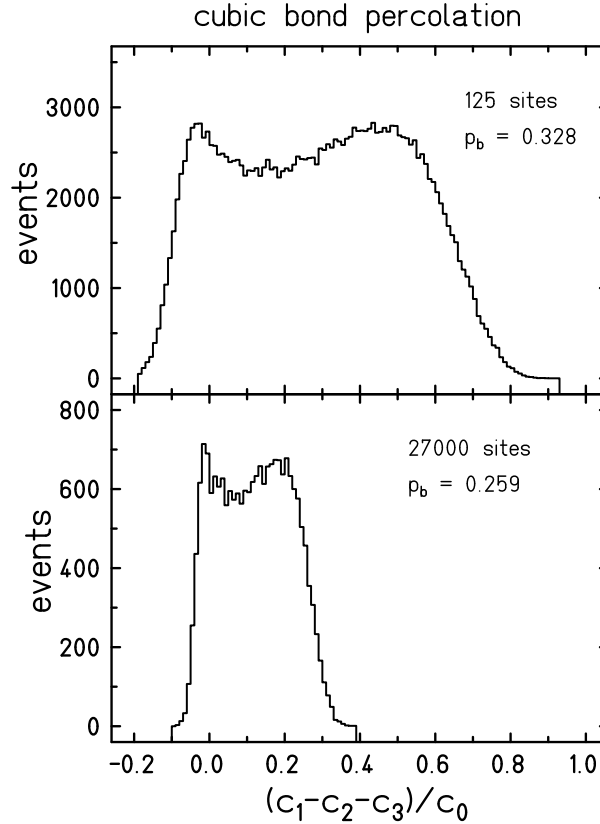


Figure 4: Examples of the distributions of the 3-fragment difference  $c_1 - c_2 - c_3$ , normalized with respect to the lattice size  $c_0 = L^3$ , as obtained with cubic bond percolation for the cases  $c_0 = 125$  sites and  $p_b = 0.328$  (top) and  $c_0 = 27000$  sites and  $p_b = 0.259$  (bottom).

## 4 Cubic bond percolation

Percolation models have been quite successfully used for describing the properties of nuclear fragmentation [17,24-28] including the apparent critical behaviour. For the present purpose, calculations with a cubic-bond-percolation model have been performed with various lattice sizes. The critical bond parameter for this type of lattice is  $p_c^\infty = 0.249$  [7, 30]. For large lattices, in the limit of infinity, a sharp transition with the sudden appearance of an extended percolating cluster is observed for this value of the probability that a bond exists between neighbouring sites. For finite lattices, the transition is smooth (Fig. 2) and, for a lattice of 81 sites (obtained by smoothing the corners and edges of a  $5^3$  lattice for simulating the 79 charges of a Au nucleus) it is very similar to what is observed in the nuclear experiment (Fig. 1). For specific values of the bond parameter in the transition region, the distributions of the 3-cluster asymmetry  $c_1 - c_2 - c_3$  (the cluster sizes  $c_i$  are ordered in magnitude) exhibit two bumps (Fig. 4). For the smaller lattice of 125 sites, the distribution extends over a major part of the interval  $[0,1]$  that is accessible after normalization with respect to the number of sites  $c_0 = L^3$ . Also this feature is reminiscent of the result obtained for the  $^{197}\text{Au}$  fragmentation (Fig. 3).

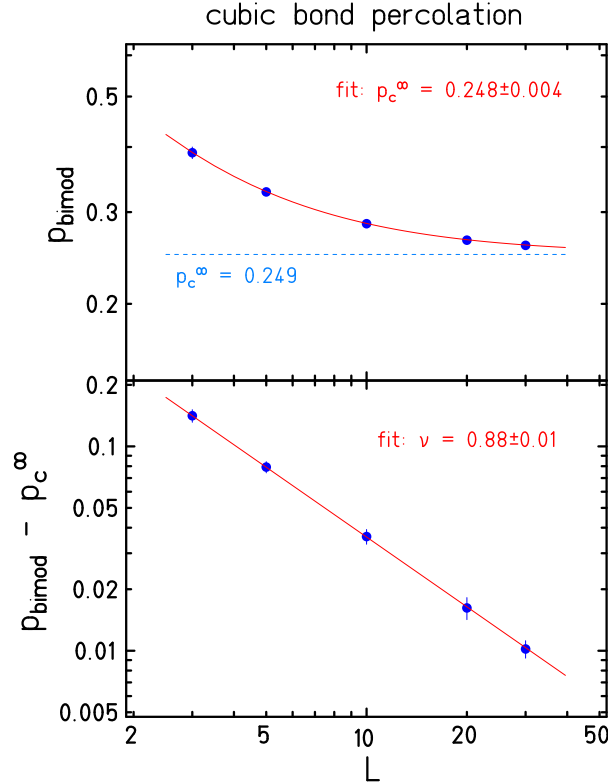


Figure 5: Bond parameter  $p_{\text{bimod}}$  for which the bimodal patterns appear most clearly (top) and difference  $p_{\text{bimod}} - p_c^\infty$  (bottom) as a function of the lattice size  $L$ . The full lines represent the results of three-parameter (top) and two-parameter (bottom, with  $p_c^\infty$  fixed) power-law fits according to Eq. 1. The dashed line indicates the location of the critical bond parameter  $p_c^\infty = 0.249$  for the infinite system [7, 30].

For the larger lattice, the distribution is still double-humped but becomes much narrower. The bond parameter  $p_{\text{bimod}}$  at which the bimodal structure is most pronounced is smaller and much closer to the critical value. Calculations performed for various lattice sizes and samples of up to 200000 events show that this variation is systematic and confirm that the law of finite-size scaling [31] is obeyed by  $p_{\text{bimod}}$ . A power law fit according to the expression

$$p_{\text{bimod}} - p_c^\infty = c \cdot L^{-1/\nu} \quad (1)$$

shows that the critical bond parameter for the infinite lattice is indeed approached by  $p_{\text{bimod}}$  (Fig. 5). A two-parameter fit with a fixed  $p_c^\infty = 0.249$  yields  $\nu = 0.88 \pm 0.01$  in agreement with the known value  $\nu = 0.88$  of the critical exponent describing the divergence of the correlation length [7].

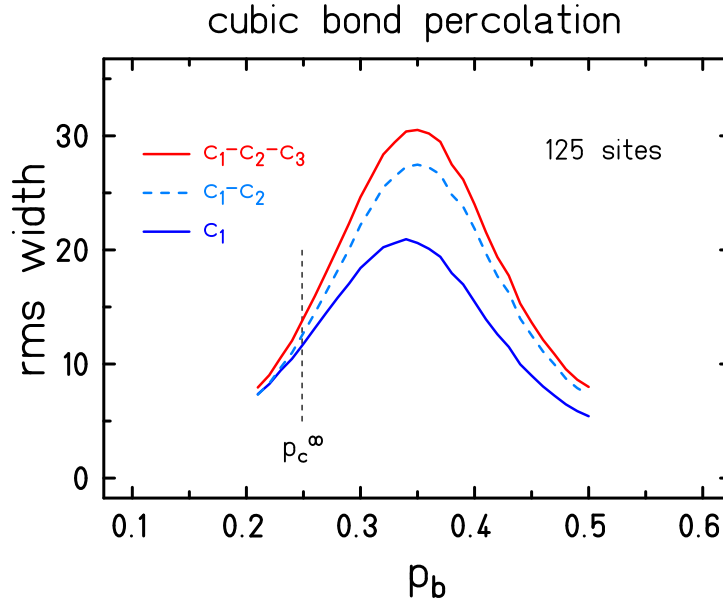


Figure 6: Root-mean-square widths of the  $c_1$  (full line, blue),  $c_1 - c_2$  (dashed), and  $c_1 - c_2 - c_3$  (full line, red) distributions as a function of the bond probability  $p_b$ .

Finite-size scaling identifies the observed phenomenon as originating from order-parameter fluctuations near the percolation phase transition. The same law with the same exponent is also valid for the locations of the maxima of the slopes of the  $\langle c_1 \rangle$  vs.  $p_b$  transition which practically coincide with  $p_{\text{bimod}}$  (cf. Fig. 2), or for the widths of the transition region [7]. The fluctuations of the largest cluster size cause corresponding fluctuations of the differences and asymmetries (Fig. 6), a property that identically appears in the fluctuation widths of the charge differences or asymmetries observed in the fragmentation of  $^{197}\text{Au}$  (Fig. 7). The existence of two bumps in the event distributions appears as a generic feature of fragmentation processes, including that modeled with percolation. The mere observation of this phenomenon can thus not be considered as providing evidence for a first-order phase transition.

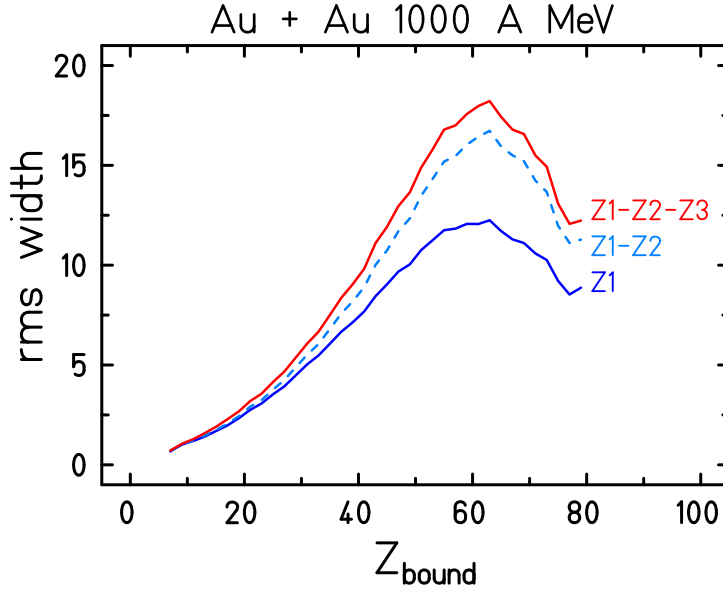


Figure 7: Root-mean-square widths of the  $Z_1$  (full line, blue),  $Z_1 - Z_2$  (dashed), and  $Z_1 - Z_2 - Z_3$  (full line, red) distributions as a function of  $Z_{\text{bound}}$ . Normalization with respect to  $Z_{\text{bound}}$  will shift the maxima to  $Z_{\text{bound}} \approx 55$ , i.e. into the center of the transition region (cf. Fig. 1).

## 5 Reaction scenarios

In classical molecular dynamics, maximum size fluctuations define a critical percolation line (Kertész line), or a critical percolation band in finite systems, in the temperature-density phase diagram [32]. The Kertész line, known from studies of the lattice-gas model [33, 34], extends from the thermodynamical critical point into the supercritical region of higher density and temperature and is considered generic for simple fluids. Its identification requires appropriate algorithms for the recognition of clusters in the dense medium. Equilibrium cluster-size distributions along the critical band exhibit a power-law behaviour and bimodality [32, 35].

It is a particular characteristic of the classical-molecular-dynamics model that the distributions of so-defined clusters do not significantly change as the systems are allowed to expand freely to a breakup point beyond which clusters can be recognized in configuration space [32]. Their properties acquired by originating from a phase space location in the critical region will be reflected in the asymptotic distributions. The reaction scenario suggested by these calculations thus links the observed percolation-like phenomena to a truly critical behaviour of large systems. The applicability of the model to nuclear fragmentation can be tested by searching for predicted non-equilibrium phenomena at breakup [32]. One of them, a considerable difference between the internal temperatures of the emerging fragments and that of the environment, is also a result of quantum-molecular dynamics (QMD [36]). The recent analysis of multifragmentation following  $^{197}\text{Au} + ^{197}\text{Au}$  collisions in the energy range 60A to 150A MeV with this model has, in particular, also shown that bimodality is observed and that the experimental asymmetry distributions of the

largest fragments are reproduced rather well with QMD [36].

On the other hand, phenomena resembling critical behaviour as it appears in large systems are also observed for equilibrium distributions of small systems generated within their coexistence zones. For the lattice-gas model, it has been rather generally shown that the observation of scaling inside the coexistence zone is compatible with a first-order phase transition because of finite size-effects [37]. The scaling will disappear in large systems. Similar conclusions were reported by the authors of [38]. When the Statistical Multifragmentation Model was used to describe the fragmentation of relativistic  $^{197}\text{Au}$  projectiles, the experimentally observed power-law  $Z$  and bimodal  $Z_{\text{max}}$  distributions in the transition region have been reproduced with conditions below the critical point of this model [21]. These phenomena thus seem to appear naturally when viewing phase transitions in small systems through their partitioning into fragments.

An interesting experimental observation is the coincidence of several signals considered indicative of a phase transition in fragmentation data [39, 40]. Besides bimodality, this includes universal fluctuations ( $\Delta$ -scaling [6]) of the size of the largest fragment and the kinetic-energy fluctuations which have been associated with negative heat capacity [41]. Searching for a common origin, it seems most likely that they are all related to the configurational fluctuations [42, 43] to be expected in fragmentation processes and identified as finite-size effects in percolation.

## 6 Summary

Experimental results regarding the largest fragment charge and the asymmetries of the two and three largest fragments in the decays of  $^{197}\text{Au}$  projectile spectators at 1000 MeV per nucleon have been presented. The bimodal distributions at specific values of the sorting variable  $Z_{\text{bound}}$  reflect the size fluctuations of the largest fragment in the transition region between the regimes of residue production and of multifragmentation. In the reaction scenario suggested by molecular dynamics, these configurational fluctuations are related to a critical percolation region in the phase diagram which reduces to a critical percolation line (Kertész line) in large systems. In small systems, critical-like phenomena like scaling, power-law cluster distributions and bimodality are also exhibited by equilibrium distributions generated at locations within the coexistence region. The underlying configurational fluctuations, identified as finite-size effects with percolation, thus seem generic for fragmentation processes in small systems.

Stimulating discussions with X. Campi and E. Plagnol are gratefully acknowledged.

## References

- [1] D.H.E. Gross, Eur. Phys. J. A 30 (2006) 293, and in *Dynamics and Thermodynamics with Nuclear Degrees of Freedom*, ed. by Ph. Chomaz et al., Springer, Berlin Heidelberg New York, 2006.



- [2] Ph. Chomaz and F. Gulminelli, *ibid.*, p. 317.
- [3] M. Pichon et al., Nucl. Phys. A 779 (2006) 267.
- [4] M. Schmidt et al., Phys. Rev. Lett. 86 (2001) 1191.
- [5] O. Lopez, D. Lacroix, E. Vient, Phys. Rev. Lett. 95 (2005) 242701.
- [6] R. Botet et al., Phys. Rev. Lett. 86 (2001) 3514.
- [7] D. Stauffer and A. Aharony, *Introduction to percolation theory*, Taylor and Francis, London, 1992.
- [8] D.H.E. Gross, in *Proceedings of the XL1st International Winter Meeting on Nuclear Physics*, Bormio, Italy, ed. by I. Iori, A. Moroni, Ricerca Scientifica ed Educazione Permanente Suppl., vol. 120, Milano, 2003, p. 110.
- [9] M. Pichon et al., *ibid.*, p. 149.
- [10] D.H.E. Gross, in *Proceedings of the XLIIIrd International Winter Meeting on Nuclear Physics*, Bormio, Italy, ed. by I. Iori, A. Bortolotti, Ricerca Scientifica ed Educazione Permanente Suppl., vol. 124, Milano, 2005, p. 148.
- [11] D.H.E. Gross, in *Proceedings of the XLIVth International Winter Meeting on Nuclear Physics*, Bormio, Italy, ed. by I. Iori, A. Tarantola, Ricerca Scientifica ed Educazione Permanente Suppl., vol. 125, Milano, 2006, p. 212.
- [12] C. Sfienti, *ibid.*, p. 229.
- [13] E. Bonnet et al., contribution to this proceedings.
- [14] J. Pochodzalla et al., Phys. Rev. Lett. 75 (1995) 1040.
- [15] A. Schüttauf et al., Nucl. Phys. A 607 (1996) 457.
- [16] C.A. Ogilvie et al., Nucl. Phys. A 553 (1993) 271c.
- [17] P. Kreutz et al., Nucl. Phys. A 556 (1993) 672.
- [18] S. Das Gupta and A.Z. Mekjian, Phys. Rev. C 57 (1998) 1361.
- [19] Hongfei Xi et al., Z. Phys. A 359 (1997) 397; erratum in Eur. Phys. J. A 1 (1998) 235.
- [20] A. Kelić, J.B. Natowitz, K.-H. Schmidt, Eur. Phys. J. A 30 (2006) 203.
- [21] A.S. Botvina et al., Nucl. Phys. A 584 (1995) 737.
- [22] N. Buyukcizmeci, R. Ogul, A.S. Botvina, Eur. Phys. J. A 25 (2005) 57.
- [23] G. Chaudhuri and S. Das Gupta, Phys. Rev. C 75 (2007) 034603.
- [24] F. Gobet et al., Phys. Rev. Lett. 87 (2001) 203401.
- [25] X. Campi, Phys. Lett. B 208 (1988) 351.
- [26] P. Désesquelles et al., Phys. Rev. C 48 (1993) 1828.
- [27] W. Bauer and A.S. Botvina, Phys. Rev. C 52 (1995) 1760.
- [28] M. Kleine Berkenbusch et al., Phys. Rev. Lett. 88 (2002) 022701.

- [29] W. Bauer, contribution to this proceedings.
- [30] see, e.g., C.D. Lorenz and R.M. Ziff, Phys. Rev. E 57 (1998) 230.
- [31] see, e.g., W.F.J. Müller et al., in *Proceedings of the XXXIIIrd International Winter Meeting on Nuclear Physics*, Bormio, Italy, ed. by I. Iori, Ricerca Scientifica ed Educazione Permanente Suppl., vol. 101, Milano, 1995, p. 394, and references therein.
- [32] X. Campi, H. Krivine, E. Plagnol, N. Sator, Phys. Rev. C 67 (2003) 044610.
- [33] A. Kertész, Physica (Amsterdam) 161 A (1989) 58.
- [34] X. Campi and H. Krivine, Nucl. Phys. A 620 (1997) 46.
- [35] X. Campi and E. Plagnol, private communication.
- [36] K. Zbiri et al., Phys. Rev. C 75 (2007) 034612.
- [37] F. Gulminelli and Ph. Chomaz, Phys. Rev. Lett. 82 (1999) 1402.
- [38] J. Pan, S. Das Gupta, M. Grant, Phys. Rev. Lett. 80 (1998) 1182.
- [39] M.F. Rivet et al., Nucl. Phys. A 749 (2005) 73c.
- [40] B. Borderie et al., Nucl. Phys. A 734 (2004) 495.
- [41] M. D'Agostino et al., Phys. Lett. B 473 (2000) 219.
- [42] X. Campi, H. Krivine, E. Plagnol, N. Sator, Phys. Rev. C 71 (2005) 041601.
- [43] F. Gulminelli and M. D'Agostino, Eur. Phys. J. A 30 (2006) 253, and in *Dynamics and Thermodynamics with Nuclear Degrees of Freedom*, ed. by Ph. Chomaz et al., Springer, Berlin Heidelberg New York, 2006.